Liquefaction-induced Settlement and Tilting of Buildings with Spread Foundation based on Field Observation and Laboratory Experiments

Kohji Tokimatsu
Tokyo Soil Research, Co. Ltd., Tokyo, Japan
Kazuya Hino, Kyoko Ohno, Shuji Tamura
Tokyo Institute of Technology, Tokyo, Japan
Hiroko Suzuki
Chiba Institute of Technology, Chiba, Japan
Yasutsugu Suzuki
Kajima Technical Research Institute, Chofu, Tokyo, Japan

ABSTRACT
Earthquake reconnaissance studies and centrifuge experiments were made and their results were compared with those of previous studies, to examine relative importance of key parameters affecting not only the settlement but also the tilt of buildings with shallow foundations. The field observation suggested that: (1) There is a general trend in which liquefaction-induced relative settlement and tilting of shallow foundation increase with increasing number of story and aspect ratio of building but the settlement trend was likely to be site dependent; (2) When the settlement is normalized with respect to the thickness of liquefied layer, there is a general trend in which it increases with increasing number of story and aspect ratio, regardless of the site-specific conditions; and (3) The overturning of building occurred only at buildings with more than 3 stories and an aspect ratio more than about 2. The centrifuge experiments suggested that: (1) The liquefaction-induced relative settlement and tilt of shallow foundations tend to increase with increasing contact pressure and ground settlement as well as decreasing groundwater table and thickness of non-liquefied crust. The tilt angle of the building also tends to increase with increasing eccentric mass and distance ratio; and (2) The safety factors against vertical load and overturning moment are key indicators to estimate liquefaction-induced damage to building founded on rigid spread foundation.

1 INTRODUCTION

Extensive soil liquefaction occurred in reclaimed land of the Tokyo Bay area and the Tone River basin during the 2011 Tohoku Earthquakes, causing excessive settlement and titling of many wooden houses and low-rise reinforced concrete (RC) buildings founded on shallow foundations. Similar damage was also observed not only on reclaimed lands but also on natural deposits during recent earthquakes such as the 2011 Christchurch and 2016 Kumamoto earthquakes. Despite many reconnaissance and laboratory studies (e.g., Tokimatsu and Yoshimi, 1977; Ishihara, 1985; Tokimatsu et al, 1994; Yoshida et al, 2001; Santio, 2004; Dashti et al, 2010; Tokimatsu et al, 2013), it seems that the liquefaction-induced settlement of buildings with shallow foundations can be affected by various factors, the relative effects of which have not been clearly identified. In addition, most of the previous studies have concentrated only on building settlement, overlooking building tilt that is equally or even more important when considering the serviceability of the building after the quake, i.e., performance-based seismic design of buildings with shallow foundations. The objective of this paper is therefore to make an attempt to examine relative importance of key parameters affecting not only settlement but also tilt of buildings with shallow foundations founded on liquefiable soils from field observation and laboratory experiments.

2 FIELD OBSERVATION

2.1 Field Observation during Past Earthquakes

Figure 1 schematically illustrates key factors controlling liquefaction-induced settlement and tilt of a building, which have been indicated in the previous reconnaissance studies. Based on field case histories regarding the 1964 Niigata earthquake and 1G shaking

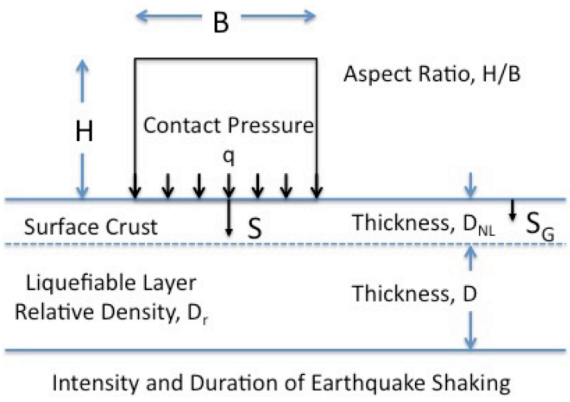

Figure 1. Key factors controlling liquefaction-induced settlement and tilt of building

table tests, Yoshimi and Tokimatsu (1977) showed that the settlement ratio normalized with respect to the thickness of liquefied layer, S/D, of RC building decreases as the ratio between building width and thickness of liquefied layer, B/D, increases. Ishihara (1985) suggested after the 1983 Nihonkai-Chubu earthquake that, if the thickness of non-liquefied crust overlying a liquefied deposit, D_{NL}, exceeds 2-3 m, would reduce liquefaction-induced damage to wooden houses during earthquakes with peak ground accelerations of the order of 2 m/s^2. Tokimatsu et al (1992) showed after the 1990 Luzon Earthquake that the contact pressure, q, and shear stress imposed by RC buildings and their adjacent buildings might have affected settlement and tilting of RC buildings. Sancio et al (2004) showed after the 1999 Kocaeli earthquake that the settlement ratio normalized with respect to foundation width, S/B, has a good correlation with the aspect ratio of RC buildings, H/B, of 4 to 6 storied. Based on reconnaissance studies regarding the 2011 Tohoku earthquakes, Tokimatsu et al (2012) showed that the tilting angles of wooden houses tend to increase with increasing liquefaction-induced ground settlement (S_G), which would probably be affected by such factors as the relative density and thickness of the liquefied layer as well as the intensity and duration of earthquake shaking.

Despite many previous field reconnaissance studies, it seems that the key factor highlighted in one study was overwhelmed by other factors or simply overlooked in other studies and that the relative importance of them has not been clearly identified. In addition, most of the previous studies have concentrated on building settlement, missing building tilt that is equally or more important when considering the serviceability of the building after the quake.

2.2 Field Observation during 2016 Kumamoto Earthquakes

The 2016 Kumamoto Earthquakes, including two major events on April 14th and 16th (M_J6.5 and M_J7.3), induced catastrophic damage to infrastructures and buildings in the source region as well as in the Kumamoto plain. Soil liquefaction and related damage also occurred mainly in the Kumamoto plain during both events with more extensively on the second one. Figures 2 and 3 show typical damage to a wooden house and a reinforced concrete building of 3 stories.

The peak ground accelerations recorded at K-NET in the Kumamoto plain were 4.24 m/s^2 and 8.51 m/s^2 for the first and second events, respectively. Despite very strong shaking, however, the area of soil liquefaction was very limited. This motivates the authors to investigate the reason why the liquefaction-induced damage was so limited and how the buildings, particularly supported on spread foundations, behaved under very strong shaking.

Figure 4 shows a map of Karikusa town and its vicinity located on the south of JR Nishi (West)-Kumamoto station, together with the investigated area encircled by a broken line. According to a geomorphological map, most of the investigated area was classified into natural levees presumably consisting of sandy soil. A total of 307

Figure 2. Liquefaction-induced tilt of a 2-story wooden house in Karikusa town

Figure 3. Liquefaction-induced settlement of a 3-story reinforced concrete building in Karikusa town

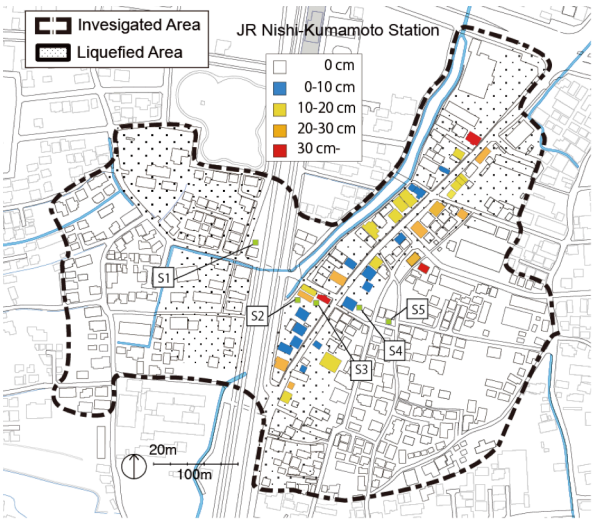

Figure 4. Distribution of liquefaction-induced settlement of buildings in Karikusa town

buildings on spread foundation were examined. Table 1 summarizes the structural type and the number of story with occurrence or nonoccurrence of soil liquefaction for the buildings investigated. About 70% are light-weight two story wooden houses.

Also shown in Figure 4 is the distribution of relative settlement of buildings in the district. Figures 5 and 6 show similar distribution of tilt angle and damage level of superstructure of buildings, which have been classified according to Tables 2 and 3. Note that houses tilting more than 6/1000 to 1/100, even without any structural damage, generally need leveling for continuous living without health problems.

Figures 4 and 5 indicate that liquefaction-induced settlement and tilting of buildings were concentrated within a narrow band along the road running from the northeast to the south, which was reportedly an old river channel about 400 years ago and later artificially reclaimed. Figure 4 also indicates that liquefaction-induced settlement of buildings relative to the ground

Table 1. Number of stories and structural type of buildings invested with sign of soil liquefaction

Type of Structure	No. of Story	Liquefaction		Total
		Yes	No	
W	1	4	66	70
	2	18	75	93
S	1	0	9	9
	2	21	83	104
	3	5	6	11
RC	1	2	0	2
	2	2	9	10
	3	3	3	6
	4	0	1	1
	5	0	1	1
Total		54	253	307

Table 2. Relation of tilt angle of building with health problem, degree of damage, and need for restoration

Tilt angle (rad)	Health Problem (AIJ, 2008)	Degree of Damage (CAO, 2011)	Need for Leveling without Health Problems
6/1000	Strong feeling of inclination		Likely
1/100	Disorders such as dizziness and headache	Partially damaged	Definitely
1/60	Physiological limit	largely damaged	
1/20		Totally damaged	

Table 3. Classification of damage to buildings (After Okada and Takai, 1999; Yoshida et al, 2001)

Damage Grade	Description
0	No damage
1	Negligible to slight damage
2	Moderate damage
3	Substantial to heavy damage
4	Very heavy damage
5	Destruction

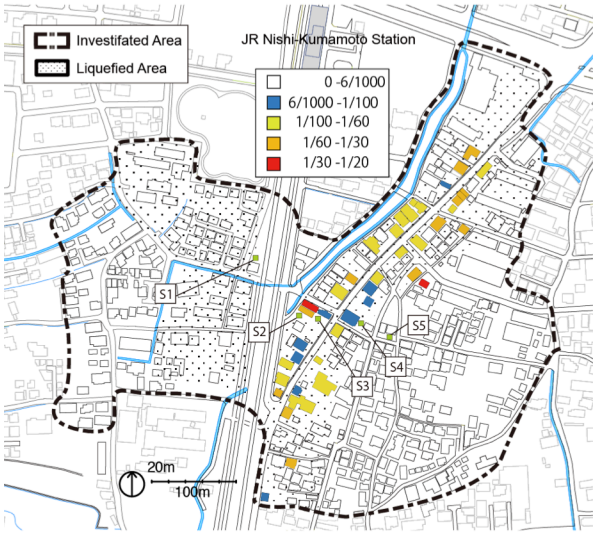

Figure 5. Distribution of liquefaction-induced tilt of buildings in Karikusa town

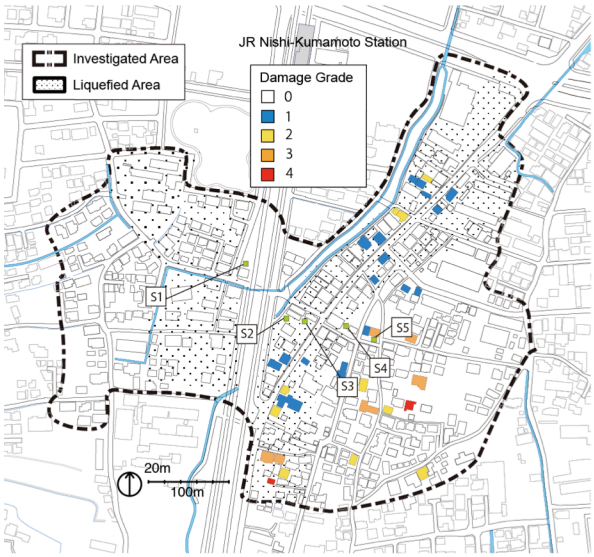

Figure 6. Distribution of damage to superstructure of buildings in Karikusa town

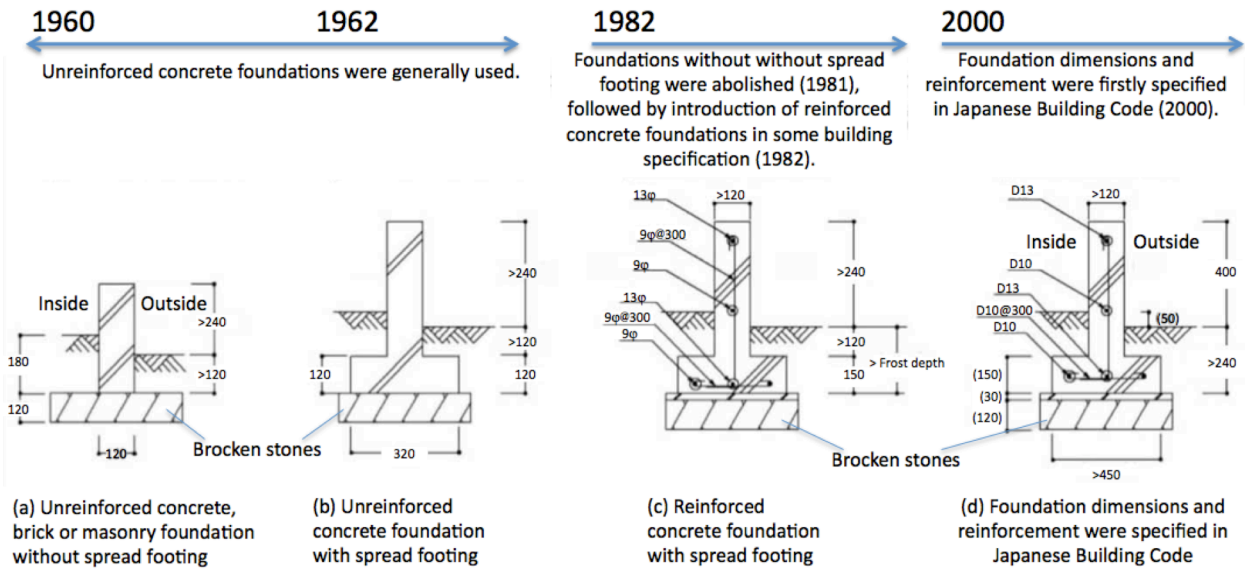

Figure 7. Historical changes in recommendation of continuous foundation design of wooden houses (in mm)

were relatively small, probably reflecting that most of the buildings were lightweight 2-story wooden houses.

Figure 6 suggests that most of vital damage to superstructure of buildings were distributed on the southeastern outside of the liquefied belt, indicating significant effects of strong ground shaking amplified through the non-liquefied near surface soil in the area. A few buildings also experienced damage to their superstructures in the southern part of the liquefied belt. All of them were very old wooden houses with unreinforced weak foundations, the damage to which during soil liquefaction would have in turn induced unacceptable deformation of their superstructures. This reflects the historical changes in design specification of continuous foundation of wooden houses as shown in Figure 7, in which more reinforcement are required with time. In exchange of reducing damage to superstructure, it seems, because of their heavier weight, new wooden houses tend to suffer more settlement than old houses.

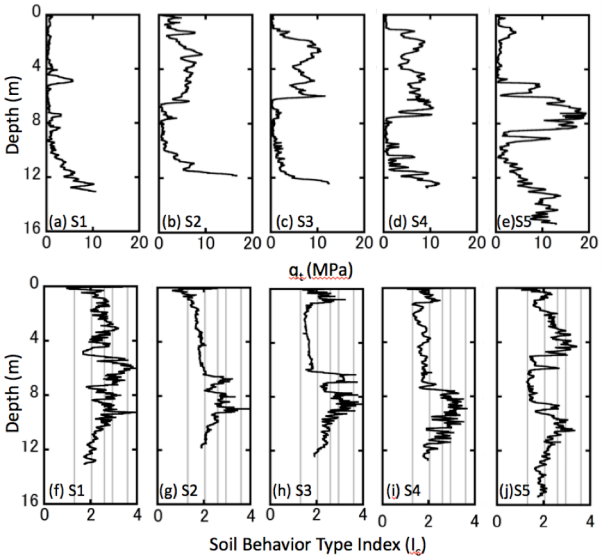

Figure 8. CPT tip resistance and soil behavior type index (I_c) at Sites 1-5

Cone penetration tests were conducted at five locations (S1 to S5) across the old river channel, with the standard penetration tests made at two sites (S3 and S5). Sites S2-S4 were located inside the liquefied belt and Sites S1 and S5 located outside as indicated in Figures 4 to 6. Figure 8 shows the distribution of cone tip resistance and normalized soil behavior type index (I_C) with depth of the five sites. Although all sites are located within the natural levees classified on the geomorphological chart of the region, sandy soils with $I_C < 2$ dominate from the ground surface to a depth of about 6 m at liquefied sites S2 to S4, while silty and clayey soils with $I_C > 2$ prevail within the same depth at non-liquefied sites S1 and S5. This suggests that the difference in liquefaction-induced damage in the region would be mainly due to the difference in near surface soil type.

2.3 Revisit to Field Case Histories of Liquefaction-Induced Damage to Buildings

Previous studies on liquefaction-induced damage to buildings during past catastrophic earthquakes are revisited to identify the difference in damage patterns, if any, between earthquakes, and to explore the key parameters having controlled general trends of damage found in all the case histories. The past case histories used together with those observed in Kumamoto, include those in Niigata during the 1964 Niigata earthquake (Yoshimi and Tokimatsu, 1977), Dagupan during the 1990

Table 4. Statistics of liquefaction-induced damage to building used from case histories in four earthquakes

Settlement (cm)	1964	1990	1999	2016
0-1	0	8	14	7
1-20	5	2	29	34
20-40	5	6	20	13
40-60	1	7	9	0
60-	21	35	1	0
Tilt Angle (rad)	**1964**	**1990**	**1999**	**2016**
0-6/1000	2	9	13	14
6-10/1000	4	5	2	5
1/100-1/60	4	1	0	16
1/60-1/20	5	26	40	19
1/20-	17	17	18	0

Luzon earthquake (Tokimatsu et al, 1994), and Adapazari during the 1999 Kocieli earthquake (Yoshida et al, 2001; Sancio et al, 2004), all of which disclosed the important information to be needed in this study.

Table 4 statistically summarizes the maximum settlement relative to the ground and tilt angle of buildings used from the case histories in the four earthquakes. The maximum relative building settlement and tilting observed in the Kumamoto earthquakes are less than 40 cm and 1/20, which are significantly less than those observed in any of the other earthquakes. This probably reflects that most of the buildings in the Karikusa town are lightweight two story wooden houses.

Figure 9 shows the relation of the maximum relative settlement with the number of stories and aspect ratio of building. There are general trends in which (1) the maximum relative settlement of building in each of the four cities tends to increase with increasing number of stories and aspect ratio but (2) the data from Niigata generally fall on the upper bound and those from the Adapazari and Kumamoto on the lower bound, with those from Dagupan in between. Such a site-specific trend is

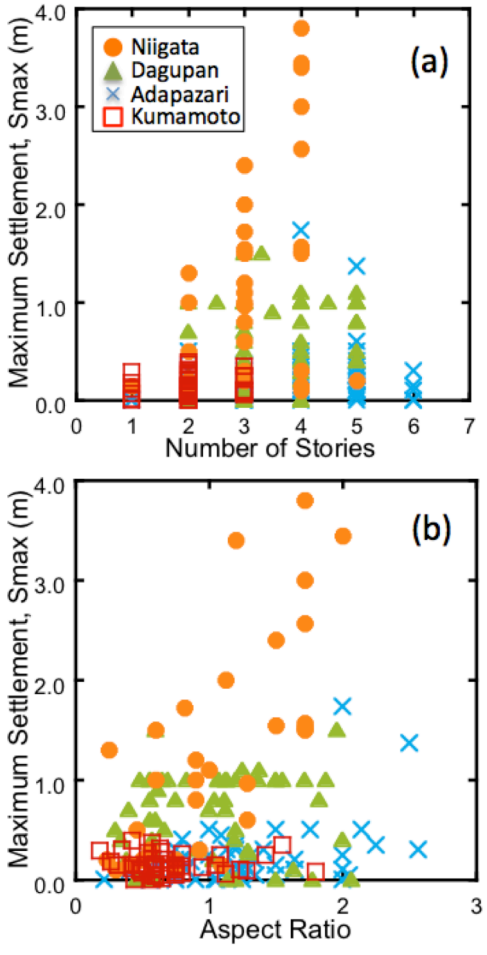

Figure 9. Relation of maximum relative settlement with number of stories and aspect ratio of building

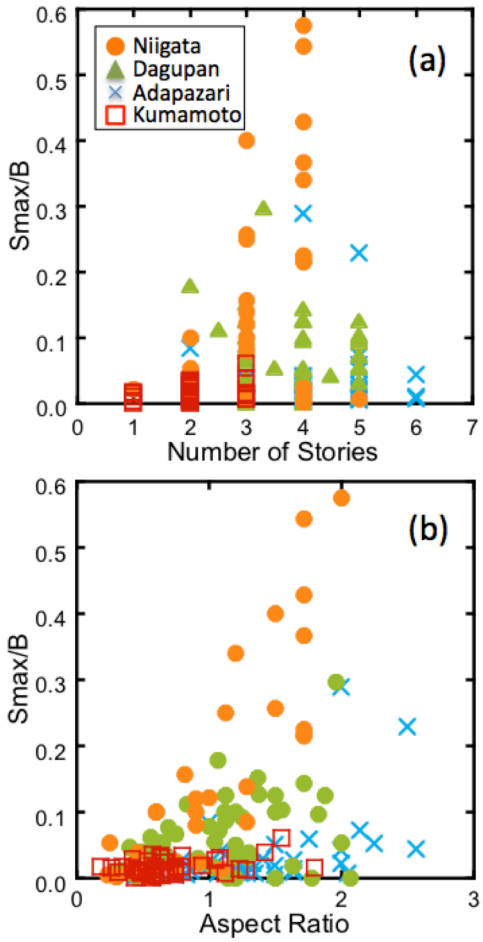

Figure 10. Relation of settlement-width ratio with number of stories and aspect ratio of building

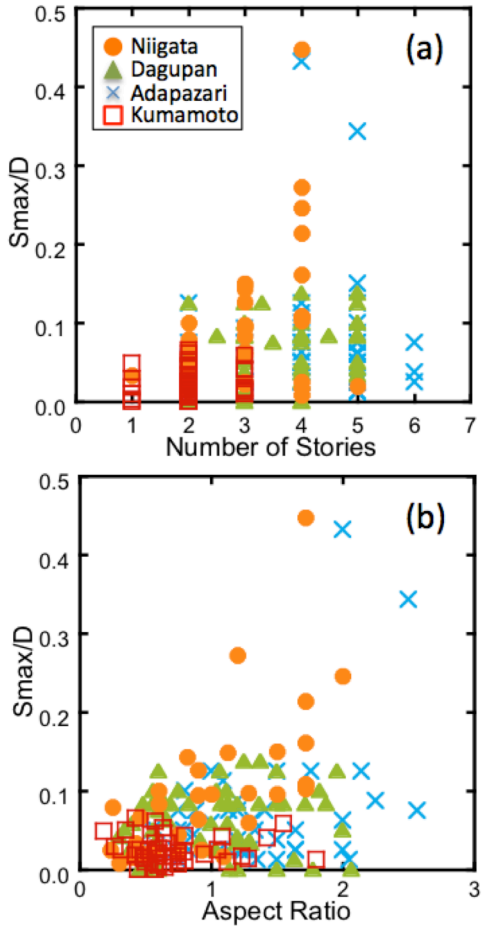

Figure 11. Relation of settlement-thickness ratio with number of stories and aspect ratio of building

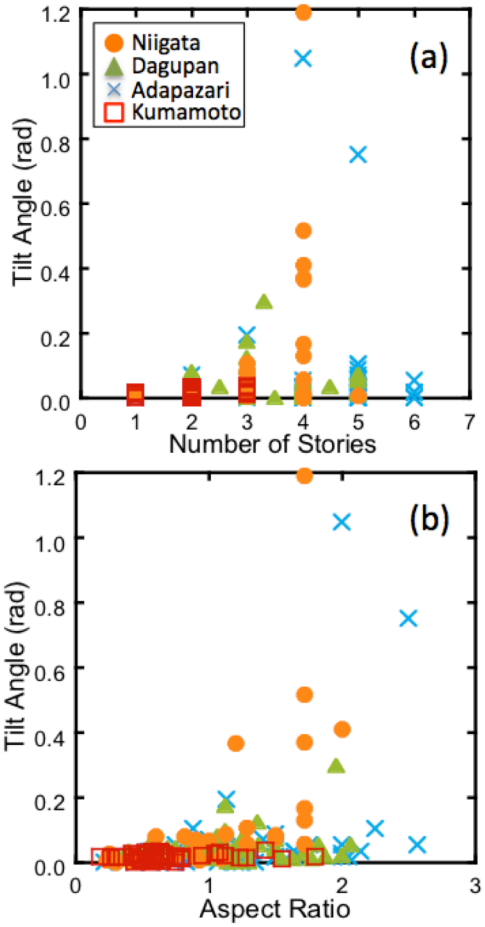

Figure 12. Relation of tilt angle with number of stories and aspect ratio of building

likely due to the difference in soil condition between the cities, e.g., the thickness, density and soil type of liquefied sand.

Based on the discussion regarding Figure 9, the relative settlement was normalized with respect to foundation width as well as the thickness of the liquefied layer, each herein defined as settlement-width ratio (S/B) and settlement-thickness ratio (S/D), respectively. Figures 10 and 11 show their relations with the number of stories and aspect ratio of building. The site-specific trend has fairly well diminished particularly when the settlement was normalized with respect to the thickness of liquefied layer.

Figure 12 shows the relation of tilt angle with the number of stories and aspect ratio of building. There is a general trend in which the tilt angle of building tends to increase with increasing number of stories and aspect ratio, with the site-specific trend observed in Figure 8 being less obvious. The figure also suggests that the large tilt leading to overturning only occurred at buildings with more than 3 stories and an aspect ratio more than about 2. Similar field observation was found elsewhere (Gazetas et al, 2004).

2.4 An Attempt to Back-Calculate Equivalent Modulus of Liquefied Layer

The general trend shown in Figure 11 may somehow relate to the immediate settlement of building supported on a liquefiable layer with a finite thickness that overlies a rigid base, as shown in Figure 13. Based on the theory of elasticity, the immediate settlement of building with rigid foundation, S, due to soil liquefaction of a layer having a finite thickness (Figure 13(a)), the Young's modulus of which has decreased from the initial value, E_o, to E (Eo >> E), may be approximated as

$$S \approx S_E(0) - S_E(D) \quad [1]$$

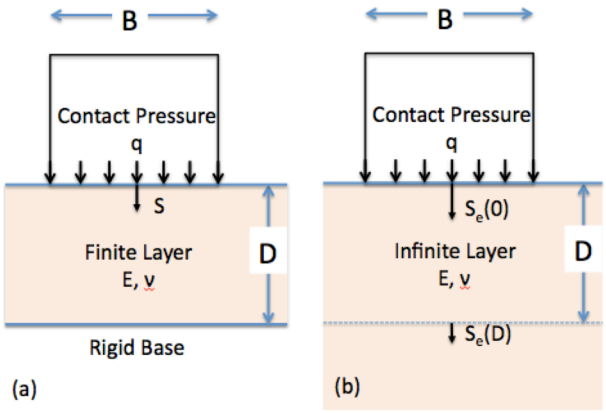

Figure 13. Estimation of settlement of building founded on a liquefiable layer with finite thickness

in which D is the thickness of the liquefied layer, and $S_E(0)$ and $S_E(D)$ are the settlements at depths zero and D below the center of the foundation resting on a layer having an infinite thickness, such as shown in Figure 13(b), and defined as

$$S_E(0) \approx a\frac{1-\upsilon^2}{E} qBI_3(0) \quad [2]$$

$$S_E(D) \approx a\frac{1-\upsilon^2}{E} qB\left[I_3(D/B) - \frac{1-2\upsilon}{1-\upsilon} I_4(D/B)\right] \quad [3]$$

in which a is constant (about 0.8), ν is the Poisson's ratio of the liquefied layer, and I_3 and I_4 are the function of non-dimensional depth, D/B, below the center of the load defined by Das (1983). Noting $I_3(0)$-$I_3(D/B)$ is approximately equal to 0.57D/B under D/B < 1.2 and assuming ν = 0.5 and a square foundation of BxB (i.e., $I_3(0)$=1.12) leads to the following:

$$S \approx \frac{qD}{3E} \quad [4]$$

The above equation suggest that, under otherwise the same condition and D/B < 1.2, the liquefaction-induced settlement would be roughly proportional to both contact pressure and thickness of liquefied layer and inversely proportional to equivalent modulus of liquefied layer, i.e., the settlement-thickness ratio of building would be roughly proportional to the contact pressure of the building. Note that, if D=B, S is nearly equal to a half of $S_E(0)$, i.e., the building settlement for an infinite layer having the same properties.

Equation 4 can be rewritten as

$$E \approx \frac{qD}{3S} \quad [5]$$

Figure 11(a) also suggests the relation between S/D and number of stories, N, defined as:

$$S/D \approx (0.0025 - 0.05)N \quad [6]$$

Assuming q = 15N (kN/m^2) for RC building and substituting Equation 6 into Equation 5 leads to the following:

$$E \approx (0.1 - 2)\mathrm{MN/m^2} \quad [7]$$

The back-calculated modulus, E, is about 0.1-2% of the elastic modulus at small strain, E_o, which is likely a reasonable range for a liquefied sand.

Although the liquefied layer may not behave as an elastic material, the above result and discussion are consistent with the trend shown in Figure 11(a) and suggest a possibility that the liquefaction-induced building settlement would be roughly estimated by knowing the contact pressure of the building as well as the thickness and equivalent modulus of the liquefiable layer.

3 OBSERVATION FROM LABORATORY EXPERIMENTS

3.1 Laboratory Observation from Past Centrifuge Experiments

Dashti et al (2010) conducted centrifuge experiments simulating the performance of reinforced concrete (RC) buildings in liquefiable soils and suggested that key parameters controlling liquefaction-induced building settlement are such factors as seismic demand, liquefaction layer thickness (D), foundation width (B), static shear stress ratio, building aspect ratio (H/B), building weight (q), and 3D drainage. Combining various building and soil conditions, more comprehensive centrifuge liquefaction experiments have been made recently (e.g., Tokimatsu et al, 2013; Hino et al, 2015). Summarized below are the test setup and procedures as well as the major findings resulting from the series of their experiments.

3.2 Test Apparatus and Procedures in Recent Centrifuge Experiments

The tests were conducted using two laminar boxes in different facilities with a centrifugal acceleration of 50 g or 25 g. Figures 14 and 15 show typical test setups in the two containers of different sizes. The small one had an inside dimension of H300mm x W220mm x L700mm, while the large one had an inside dimension of H600mm x W800mm x L1950mm. Most of the tests were run with the small container under 50 g using a scaling factor of 50. Some were run with the large container under 25 g using a scaling factor of 25. The tests with a scaling factor of 25 simulated proto-type configurations, while

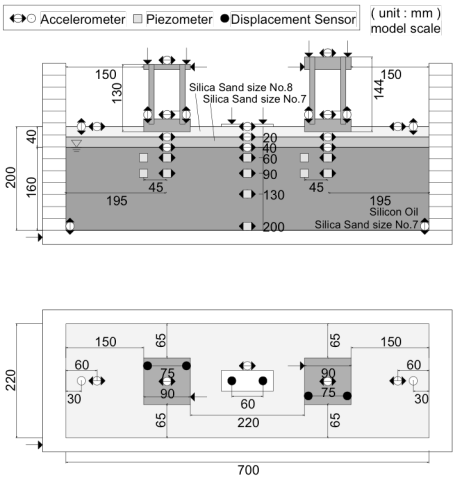

Figure 14. Test setup for Test A

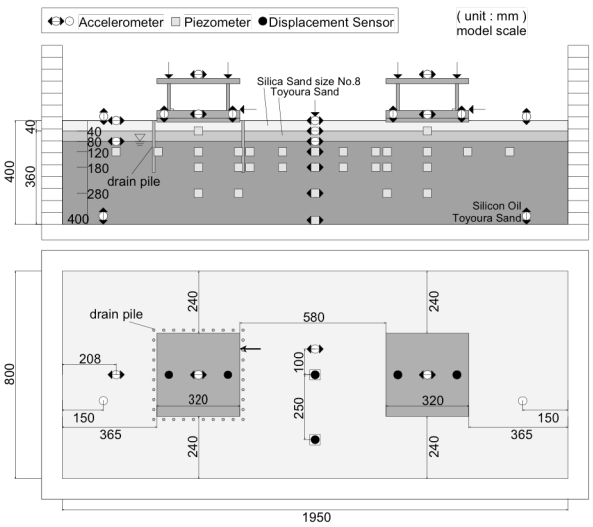

Figure 15. Test setup for Test O

those with a scaling factor of 50 was a half scale model of the prototype model. The purpose of using different scaling factor and model size was to minimize time and cost involved in the tests, while examining the effects of both scaling law and side boundaries of the smaller container closely located to the building. Henceforth, the test apparatus and results, except for the characteristics of sands used, were shown in the prototype scale.

Table 5. List of centrifuge tests

Test ID	Model ID	Building ID	Soil ID	Number of Shaking	Centrifugal Acc.
A	5S_2L	5S	2L	5	50G
	7S_2L	7S			
B	5S_3L$_2$	5S	3L$_2$	6	
	7S_3L$_2$	7S			
C	5S_4L$_2$	5S	4L$_2$	6	
	7S_4L$_2$	7S			
D	5E_3L$_2$	5E	3L$_2$	4	
	9S_3L$_2$	9S			
E	7L_3L$_2$	7L	3L$_2$	5	
F	7S_3LD	7S	3LD	4	
	9S_3LD	9S			
G	7S_3DL	7S	3DL	8	
	9S_3DL	9S			
H	2S_1L	2S	1L	3	
I	2S_1L*	2S	1L	2	
J	2S_3L	2S	3L	3	
K	2S_4L	2S	4L	3	
L	2L_1L	2L	1L	2	
M	2L_3L	2L	3L	1	
N	2L_3L*	2L	3L	3	
O	2L'_2M	2L'	2M	5	25G
P	2L'_2M'	2L'	2M	3	

Table 5 summarizes the list of tests used in this study. Tests A to G were newly conducted for this study, while Tests H to P were those previously performed by Tokimatsu et al (2013) and Hino et al (2015) to investigate the effects of drain pipes on the performance of building. In either case, either one or two buildings were set on liquefiable sand deposits, with the groundwater depth, building dimensions, and maximum input acceleration being varied. Only one building each is listed in Cases H to P, because the drain piles, which are not the subject of this paper, were inserted around the other building to examine their effects on settlement and tilting of the building. Altogether, 16 tests were run with total of 22 buildings supported on spread foundation.

Table 6 summarizes the characteristics of 8 buildings with different foundation width, contact pressure, height of gravity center, and load eccentricity ratio. The two letters of building ID in turn reflect the contact pressure (2:

Table 6. List of building models

Building ID	Contact Pressure (kN/m^2)	Height of Gravity Center (m)	Foundation Width (m)	Mass Eccentric Ratio
2S	20	2.5	4.5	0.04
2L	20	2.5	9.0	0.04
2L'	20	2.5	8.0	0.04
5S	50	2.5	4.5	0.04
5E	50	2.5	4.5	0.10
7S	70	3.5	4.5	0.04
7L	70	3.5	9.0	0.04
9S	90	4.5	4.5	0.04

20kN/m^2; 5: 50kN/m^2; 7: 70kN/m^2; and 9: 90kN/m^2) and foundation width and eccentricity ratio (S: 4.5m and 0.04; L: 9.0m and 0.04; L': 8.0m and 0.04; and E: 4.5m and 0.10). The natural periods of building were 0.3-0.4 s for 2S, 2L and 2L'; 0.15 s for 5S and 5E; 0.2 s for 7S and 7L; 0.25s for 9S. The contact pressure, height of gravity center, and natural period of buildings 2S, 2L, and 2L' corresponded to those of two-story wooden houses and of the remaining buildings to those of 2 to 4 story RC buildings. The roof floor and foundation of each model building were made of monocast (MC) nylon or duralumin, both of which were tightly fixed to the ends of the column walls made of either MC nylon, ultra super duralumin, or aluminum. The embedded depths of foundation were 0.50m for Tests A to G, 0.15m for Tests H to N, and 0.25m for Tests O and P.

Table 7 summarizes characteristics of 9 model grounds with different groundwater table and different stratification of soil density. The first letter of Soil Model ID reflects groundwater table (1: 1m; 2: 2m, 3: 2.5m; and 4: 4.0m), with the rest (one to three letters) representing the variation of relative density (L: 50%; M: 60-65%; and D: 90%) with depth below the groundwater table.

The model ground in Tests A to N was prepared with air-pluviation method in the small laminar box using Silica sand #8 (D_{50} = 0.096 mm, e_{max} = 1.40, e_{min} = 0.78) for the top 1m and Silica sand #7 (D_{50} = 0.16 mm, e_{max} = 1.18, e_{min} = 0.69) below that depth, with silicon oil with 50 cst as the pore fluid. The coefficient of permeability of the liquefiable layer below the groundwater table (Silica sand #7) with 50cst silicon oil was 2.8x10^{-4} cm/s. To investigate effects of permeability of soil layer, two Tests I and N were conducted with 200 cst silicon oil, which are indicted with asterisk in Table 7.

The model ground in Tests O and P was made in the large laminar box using the same sand for the top 1m and Toyoura sand (D_{50} = 0.21 mm, e_{max} = 0.99, e_{min} = 0.63) below that depth, with silicon oil having 25 cst as the pore fluid. In both cases, once the height of the sand layer reached the groundwater table specified in Table 5, it was saturated using silicon oil under vacuum. Subsequently, the sand layer above the groundwater table was further prepared by air-pluviation method. After completion of sand layer, either one or a pair of building models was placed on the ground with a specified embedment depth. During the preparation of soil building models, accelerometers, pore water pressure transducers and displacement meters were installed in and on the soil as well as on the buildings.

An artificial ground motion called Rinkai (Tokimatsu et a, 2013; Hino et al, 2015) was used as an input motion in the longitudinal direction of the laminar box. The outputs from the installed sensors were recorded until the excess pore pressure in the ground had dissipated completely. This shaking and observation process was repeated up to several times until one of the displacement sensors for measuring settlement and tilting of the building became out of scale. The maximum acceleration was adjusted to 4.0 m/s^2 for the first flight, 2.0 m/s^2 for the second, and 4.0 m/s^2 thereafter. This paper discusses the results mainly from the first flight and partly from the latter ones.

Table 7. List of soil modes

Soil ID	Water Table (m)	Relative Density (%)
1L	1.0	50 (0-10m)
3L	2.5	50 (0-10m)
4L	4.0	50 (0-10m)
2L	2.0	65 (0-2.0m), 50 (2.0-10m)
2M	2.0	60 (0-10m)
$3L_2$	2.5	65 (0-2.5m), 50 (2.5-10m)
$4L_2$	4.0	65 (0-4.0m)
3LD	2.5	65 (0-2.5m), 50 (2.5-6.5m), 90 (6.5-10m)
3DL	2.5	80 (0-1.0m), 90 (1.0-2.5m), 90 (2.5m-6.0m), 50 (6.0-10m)

3.3 Effects of Contact Pressure, Thickness of Non-Liquefiable layer and Soil Layering

Figure 16 compared the centrifuge data ranges with those observed in the field (Figure 9(a) and 12(b)). The areas

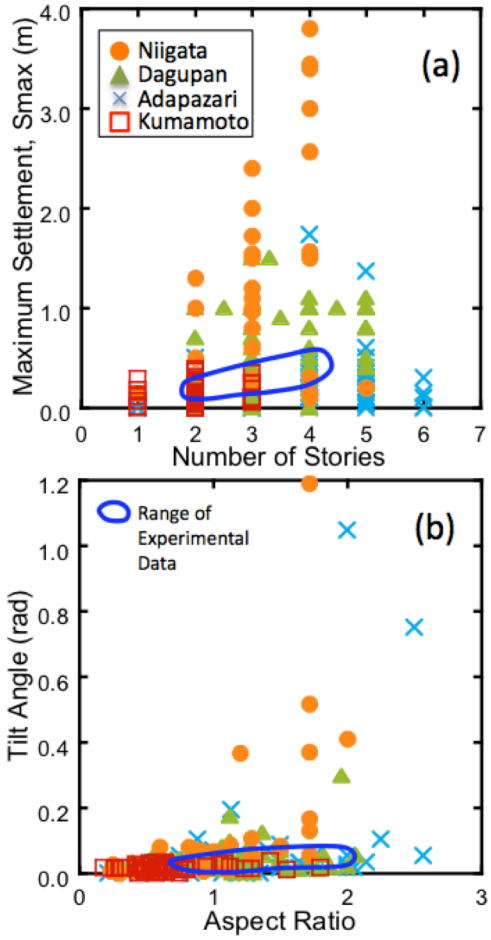

Figure 16. Comparison of centrifuge data ranges with those observed in the field

encircled in solid lines correspond to the test results from the centrifuge experiments. The test results are likely consistent with the field observation but fall on the lower side of the field data, probably due to the difference in soil conditions including density between field and laboratory.

Figure 17 shows the relations of contact pressure with the absolute settlement, relative settlement, and tilting angle of all building models on soil models 3L2, i.e., the same groundwater table and soil density, after the excess pore water pressure in the ground had dissipated completely. The solid line in the figure indicates the trend of the results with the same foundation width and eccentricity ratio indicated in solid symbols. The figure suggests that, under otherwise the same conditions, all the absolute and relative settlements, and the tilting angle of building tend to increase with increasing contact pressure of the building. In addition, a comparison of the two test results with different foundation widths in the figure (solid and open circles) suggests that both absolute and relative settlements tend to increase with increasing foundation width. Also, a comparison of the test results with different eccentricity ratios (solid and open triangles) confirms that the tilt angle of building tends to increase with increasing eccentricity ratio.

Figure 18 shows the relations of groundwater table with the absolute and relative settlements as well as the tilting angle of all building models 7S tested. The solid symbols and line in the figure represent the test results with a homogeneous soil deposit having a relative density of 50% below the groundwater table. The figure suggests that, under otherwise the same conditions, all the absolute settlement, relative settlement, and tilt angle of building tend to decrease with increasing groundwater table. In addition, if the groundwater table becomes 4 m, the relative settlement and tilting angle of building becomes negligible small even though the liquefaction-induced absolute settlement of the building occurs. This means that the building settled together with the ground probably due to the thick non-liquefied crust overlying the liquefiable sand.

The open triangles in the figure correspond to the tests results with soil models stratifying into loose and dense layers below the groundwater table. The down triangle has a loose sand layer underlain by a dense sand layer (3LD), while the up triangle has a dense sand layer underlain by a loose sand layer (3DL). A comparison of the test results with different density configuration (solid and open symbols) suggests that the reduction in loose layer thickness immediately below the groundwater table (up triangle) would have insignificant effects on reducing the absolute and relative settlement, and tilt angle of building. The increase in non-liquefied layer thickness immediately below the groundwater table, in contrast, does have significant effects on reducing absolute and relative settlements of building.

Figure 19 shows the relations of the non-liquefied crust thickness with the absolute and relative settlements and the tilt angle of all building models 7S in the first and second flights, in terms of the settlement of level ground. The figure confirms that the reduction in non-liquefied crust generally increases the settlement and tilt of building and that such a trend becomes significant with increasing

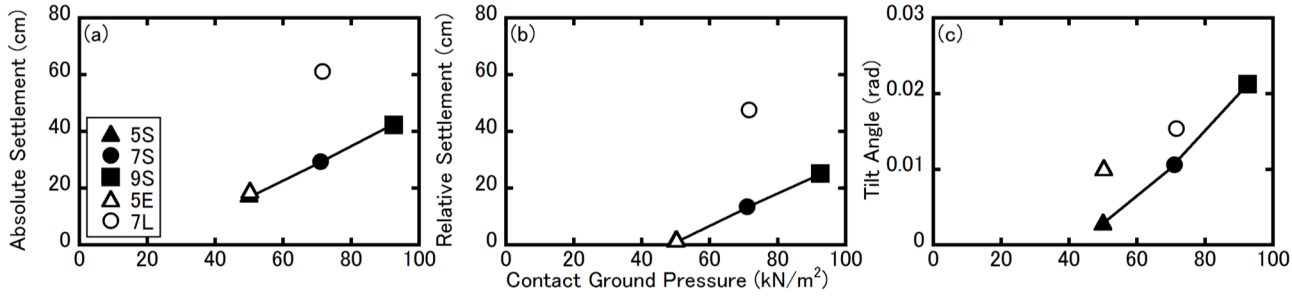

Figure 17. Relations of contact pressure with absolute settlement, relative settlement, and tilting angle of all buildings founded on soil models 3L

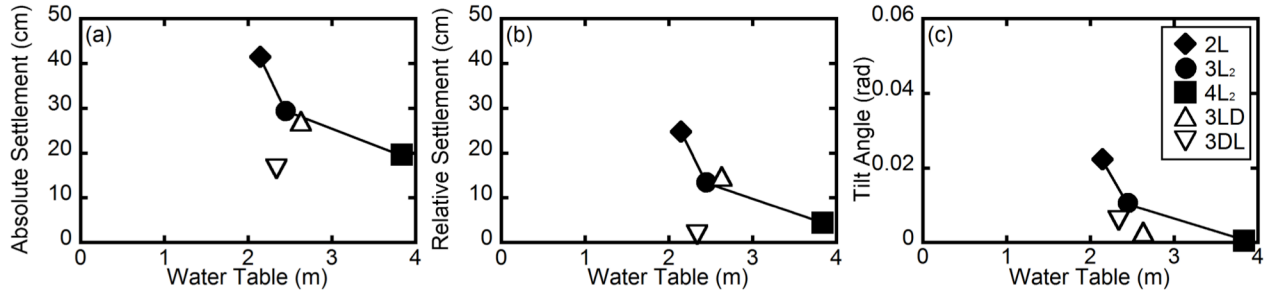

Figure 18. Relations of groundwater table with absolute and relative settlements as well as tilting angle of all building models 7S

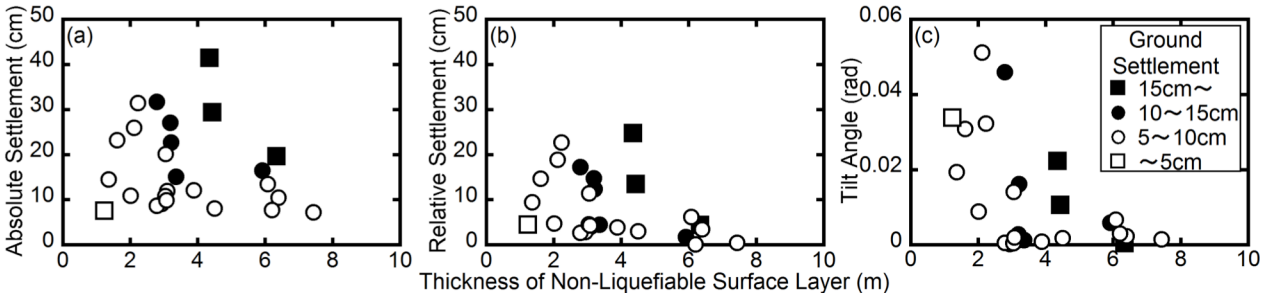

Figure 19. Relations of the non-liquefied crust thickness with absolute and relative settlements and tilt angle of all building models 7S in the first and second flights, in terms of the settlement of level ground

liquefaction-induced settlement of the level ground, i.e., liquefaction severity. This is consistent with the field observation during the 2011 Tohoku earthquakes reported by Tokimatsu et al (2012).

3.4 Safety Factors Against Vertical Load and Overturning Moment

To evaluate the liquefaction-induced damage to building affected by various key factors in a slightly more qualitative manner, Figure 20 shows the equilibrium of vertical force and rotational moment of a building founded on a non-liquefiable layer having of a thickness of Z. Assuming that only the shear force of the non-liquefied crust can act against the vertical force and the overturning moment from the building, the safety factor with respect to the vertical force equilibrium F_{sw} is given as

$$F_{SW} = R_W / L_W \quad [8]$$

in which R_w is the resisting force and L_w is the entire vertical force of the building; both defined respectively as

$$R_W = \int_0^Z (K\sigma_V' \tan\varphi)\, dz \times (2B + 2L) \quad [9]$$

$$L_W = (m_1 + m_2 + m_e)g \quad [10]$$

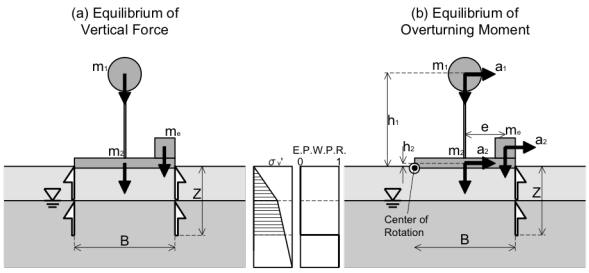

Figure 20. Equilibrium of vertical force and rotational moment of a building founded on a non-liquefiable layer having of a thickness of Z

in which K is the coefficient of earth pressure; σ_V' is the effective vertical stress; Z is the thickness of the non-liquefied surface layer; φ is the internal friction angle of the non-liquefiable soil; B is the building width in the exciting direction; L is the building length in the orthogonal direction; m_1, m_2 and m_e are the masses of superstructure, foundation and eccentric portion; and g is the acceleration of gravity.

The safety factor with respect to the dynamic overturning moment F_{sm} with respect to the center of rotation shown in Figure 7 is given as

$$F_{SMe} = R_{Me} / L_{Me} \quad [11]$$

in which R_{Me} is the resisting moment and L_{Me} is the overturning moment; both defined respectively as

$$R_{Me} = \int_0^Z (K\sigma_V' \tan\varphi)\, dz \times (B + L)B \quad [12]$$

$$L_{Me} = m_1 a_1 h_1 + (m_2 + m_e) a_2 h_2 + (m_1 + m_2) gB/2 + m_e g(B/2 + e) \quad [13]$$

in which a_1 and a_2 are the maximum accelerations after liquefaction of the superstructure and foundation, h_1 and h_2 are the heights of the center of gravity of superstructure and foundation, and e is the horizontal distance between the centers of the foundation and the eccentric mass.

Figure 21 shows the relationship between the safety factor against vertical force and the absolute and relative settlements. There is a well-defined trend in which both absolute and relative settlements decrease with increasing safety factors, with the latter becoming negligible small if the safety factor against vertical force exceeds one.

Figure 22 shows the relationship between the safety factor against dynamic overturning moment and the tilt angle of the building. The tilt angle of the building, although scattered, by and large decreases as the safety

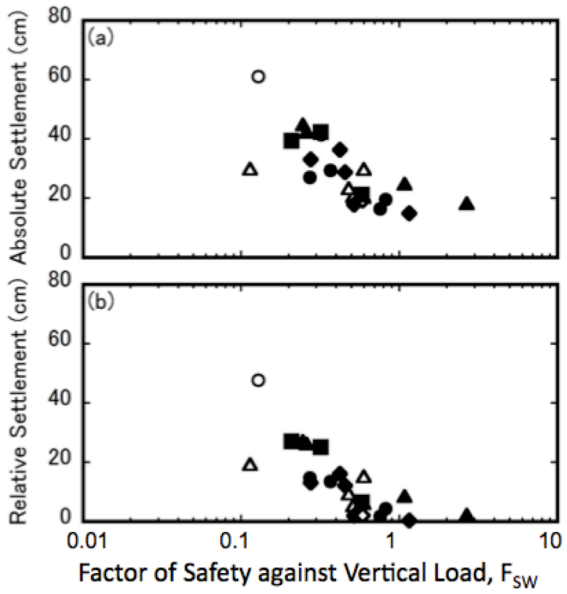

Figure 21. Relation of safety factor against vertical force with absolute and relative settlements

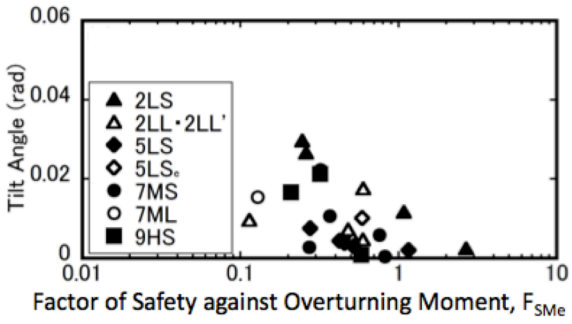

Figure 22. Relation of safety factor against overturning moment with tilt angle of building

factor against overturning moment increases and gets almost zero if it exceeds one.

The fairly well defined trends in Figures 21 and 22 suggest that, although most of the data are based on the tests run with loose sandy deposit having a relative density of 50 %, the safety factors against vertical load and overturning moment are promising indicators to estimate liquefaction-induced damage to building founded on rigid shallow foundations.

4 CONCLUDING REMARKS

The field reconnaissance survey made in Karikusa town, Kumamoto, after the 2016 Kumamoto earthquakes showed the following:

1) Despite the strong ground shaking, the liquefaction-induced damage to building in the region was limited within a narrow band, which was reportedly an old river channel about 400 years ago and later artificially reclaimed.

2) Difference in soil behavior between inside and outside the liquefied zone was mainly due to the difference in soil type between the two, i.e., sandy soils with $I_c < 2$ dominate inside, while clayey soils with $I_c > 2$ prevail outside.

3) The liquefaction-induced relative settlement and tilting of building in the liquefied belt were generally smaller than those observed in other earthquakes, reflecting that most of the buildings in the region was lightweight wooden houses of 2 stories.

4) A few old wooden houses in the liquefied belt experienced damage to their superstructures, which would have resulted from damage to their unreinforced weak foundation based on an old specification.

The revisiting of previous earthquake reconnaissance studies on liquefaction-induced damage to buildings suggested the following:

1) There was a general trend in which liquefaction-induced relative settlement and tilting increase with increasing number of story and aspect ratio of building but the settlement trend is likely to be site dependent.

2) When the settlement was normalized with respect to the thickness of liquefied layer, there is a general trend in which it increases with increasing number of story and aspect ratio, regardless of the site-specific conditions.

3) The overturning of building occurred only at buildings with more than 3 storied and an aspect ratio more than about 2.

The centrifuge shaking table tests conducted to investigate the key factors affecting liquefaction-induced damage to buildings with spread foundations suggested the following:

1) The liquefaction-induced absolute and relative settlements and tilt angle of building tend to increase with increasing contact pressure and ground settlement as well as decreasing groundwater table and thickness of non-liquefied crust. The tilt angle of the building also tends to increase with increasing eccentric mass and distance ratio.

2) The safety factors against vertical load and overturning moment are key indicators to estimate liquefaction-induced damage to building founded on rigid spread foundation.

Since the conclusions drawn from the centrifuge tests are based on a limited set of soil-building conditions and ground motion characteristics, further studies are therefore required to examine whether the above conclusions are adequate under more various conditions including the duration, frequency content and strong pulse direction of the ground motions as well as the interaction between adjacent buildings.

REFERENCES

Architecture Institute of Japan (AIJ), 2008. Recommendations for Design of Small Building Foundations, 335pp.

Cabinet Office, Government of Japan (CAO). 2011. Guideline for certifying liquefaction-induced damage to building, Action for the Great Tohoku Earthquakes, http://www.bousai.go.jp/taisaku/pdf/jiban_unyou.pdf

Das, B.M. 1983. Advanced Soil Mechanics, McGraw-Hill Book Company, 511pp.

Dashti, S., Bray, J. D., Pestana, J. M., Riemer, M. R., and Wilson, D. 2010**.** Mechanisms of Seismically-induced Settlement of Buildings with Shallow Foundations on Liquefiable Soil, *Journal of Geotechnical and Geoenvironmental Engineering*, 136**(**1**)**; 151–164.

Gazetas, G., Apostolou, M. and Anastasopoulos, J. 2004. Seismic Bearing Capacity Failure and Overturning of 'Terveler' Building in Adapazari, 1999, *Fifth International Conference on Case Histories in Geotechnical Engineering*, New York, USA, 5pp.

Hino, K., Tokimatsu, K., Suzuki, Y., Suzuki, H. 2015. Effects of groundwater depth on differential settlement of wooden houses during soil liquefaction, *Sixth ICEGE,* Christchurch, New Zealand, 8pp.

Ishihara, K. (1985): Stability of natural deposits during earthquakes, Proc., 11th ICSMFE, Vol. 1, 321-376.

Okada, S. And Takai, N. 1999. Classification of Structural Types and Damage Patterns of Buildings for Earthquake Field Investigation, *Journal of Structure and Construction Engineering*, 524, 65-72.

Sancio, R., Bray, J. D., Durgunoglu, T., and Onalp, A. 2004. Performance of buildings over liquefiable ground in Adapazari, Turkey, *13th World Conf. on Earthquake Engineering*, Vancouver, Canada, Paper No. 935.

Tokimatsu, K., Kojima, J., Kuwayama, S., Abe, A., and Midorikawa, S. 1994. Liquefaction-induced Damage to Buildings in 1990 Luzon Earthquake, *Journal of Geotechnical Engineering*, 120**(2)**; 290–307.

Tokimatsu, K., Tamura, S., Suzuki, H., and Katsumata, K. 2012. Building Damage Associated with Geotechnical Problems in the 2011 Tohoku Pacific Earthquake, *Soils and Foundations*, 52(5); 956-974.

Tokimatsu, K., Tohyama, K., Suzuki, H. and Suzuki, Y. 2013. Experimental Investigation on Dewatering and Drainage Methods to Mitigate Liquefaction Damage to Existing Houses, *10th Int. Conf. on Urban Earthquake Engineering*, Tokyo, Japan, 543-548.

Yoshida, N., Tokimatsu, K., Yasuda, S., Kokusho, T., Okimura, T., 2001. Geotechnical Aspects of Damage in Adapazari City during 1999 Kocaeli, Turkey Earthquake, *Soils and Foundations*, 41(4); 25-45.

Yoshimi, Y., and Tokimatsu, K. 1977. Settlement of Buildings on Saturated Sand during Earthquakes, *Soils and Foundations*, 17**(**1**)**; 23–38.